



## Research article

# A novel model of urosepsis in mice developed by ureteral ligation and injection of *Escherichia coli* into the renal pelvis

Haopu Hu<sup>a</sup>, Qiuxia Yan<sup>b</sup>, Xinwei Tang<sup>a</sup>, Shicong Lai<sup>a</sup>, Ziyu Qin<sup>c</sup>, Tao Xu<sup>a</sup>, Hong Zhang<sup>c,\*,\*\*</sup>, Hao Hu<sup>a,\*</sup>

<sup>a</sup> Department of Urology, Peking University People's Hospital, Beijing, China

<sup>b</sup> Department of Urology, Huizhou First People's Hospital, Huizhou, Guangdong, China

<sup>c</sup> State Key Laboratory of Vascular Homeostasis and Remodeling, The Institute of Cardiovascular Sciences, School of Basic Medical Sciences, Peking University Health Science Center, Beijing, China

## ARTICLE INFO

## Keywords:

Urosepsis

Mice

Animal model

*Escherichia coli*

Pathophysiology

## ABSTRACT

Despite extensive investigations, urosepsis remains a life-threatening and high-mortality illness. The absence of widely acknowledged animal models for urosepsis prompted this investigation with the objective of formulating a replicable murine model. Eighty-four adult male C57BL/6J mice were arbitrarily distributed into three cohorts based on the concentration of the *Escherichia coli* (*E. coli*) solution administered into the renal pelvis: Sham, Low-grade sepsis ( $1.0 \times 10^8$  cfu/mL), and High-grade sepsis ( $1.0 \times 10^9$  cfu/mL). By fabricating a glass needle with a 100  $\mu$ m outer diameter, bacterial leakage during renal pelvic injection was minimized. After the ureteral ligation, the mice were injected with this needle into the right renal pelvis (normal saline or *E. coli* solution, 1 ml/kg). Ten days post after *E. coli* injection, the mortality rates for the Low-grade sepsis and High-grade sepsis groups stood at 30 % and 100 %, respectively. Post-successful modeling, mice in the urosepsis cohort exhibited a noteworthy reduction in activity, body temperature, and white blood cell count within a 2-h timeframe. At the 24-h mark post-modeling, mice afflicted with urosepsis displayed compromised coagulation functionality. Concurrently, multiple organ dysfunction was confirmed as evidenced by markedly elevated levels of inflammatory factors (IL-6 and TNF- $\alpha$ ) in four distinct organs (heart, lung, liver, and kidney). This study confirmed the feasibility of establishing a standardized mouse model of urosepsis by ureteral ligation and *E. coli* injection into the renal pelvis. A primary drawback of this model resides in the mice's diminished blood volume, rendering continuous blood extraction at multiple intervals challenging.

## 1. Introduction

Sepsis is categorized as a perilous pathological condition whereby the dysregulated immune response to an infection results in organ dysfunction [1]. Moreover, urosepsis is an equivalent affliction that emanates from a urinary tract infection, accounts for 9–31 % of sepsis and has a mortality of 20–40 % [2,3]. The gravity of these medical enigmas is widely known among hospitals and healthcare

\* Corresponding author.

\*\* Corresponding author.

E-mail addresses: [zhanghong@bjmu.edu.cn](mailto:zhanghong@bjmu.edu.cn) (H. Zhang), [huhao@bjmu.edu.cn](mailto:huhao@bjmu.edu.cn) (H. Hu).

<https://doi.org/10.1016/j.heliyon.2024.e25522>

Received 28 July 2023; Received in revised form 25 January 2024; Accepted 29 January 2024

Available online 1 February 2024

2405-8440/© 2024 Published by Elsevier Ltd.

This is an open access article under the CC BY-NC-ND license

(<http://creativecommons.org/licenses/by-nc-nd/4.0/>).

professionals worldwide. However, the pathophysiological mechanism of sepsis is extremely complex and is not fully understood today. Presently, it is posited that bacterial or bacterial cell wall components function as pathogen-associated molecular patterns (PAMPs), binding to pattern recognition receptors (PRRs) on the surfaces of macrophages, neutrophils, endothelial cells, or urothelial cells in the presence of infection [4,5]. The transcription factor NF- $\kappa$ B orchestrates the generation of pro-inflammatory cytokines such as IL-6, IL-12, and TNF- $\alpha$ . The production of additional mediators (chemokines, prostaglandins, thrombin, and leukotrienes) contributes to the "inflammatory cytokine storm." Concurrently or subsequently, heightened secretion of anti-inflammatory cytokines and coinhibitory molecules, diminished expression of human leukocyte antigen-DR (HLA-DR), immunocyte apoptosis, and the proliferation of regulatory cells culminate in immunosuppression, augmenting susceptibility to opportunistic infections—the primary etiology of adverse prognosis in septic patients [6].

Endotoxin or bacterial injection, ascending colon stent peritonitis (CASP), and cecal ligation and puncture (CLP) are prevailing sepsis models [7]. Among these, the mouse CLP model in the realm of experimental sepsis has ascended to eminence, currently recognized as the quintessential benchmark for sepsis research. Nevertheless, there exists a discernible scarcity of widely employed and standardized animal models pertaining to urosepsis. Certain scholars revealed that a urosepsis model can be established via intrarenal infusion of *Escherichia coli* into New Zealand rabbits' renal pelvis [8,9]. Recently, some scholars have attested to the efficacy of the Wistar rat model for urosepsis [10]. Existing animal models of urosepsis involve ligating the distal ureter while simultaneously injecting *Escherichia coli* through the proximal ureter, inducing renal pelvis hypertension and bacterial translocation from the collecting system into the bloodstream. This approach effectively mirrors the clinical pathogenic mechanisms of urosepsis. However, for New Zealand rabbits or Wistar rats, due to the absence of specific antibodies or transgenic animals, subsequent foundational mechanistic studies are impeded. Consequently, only physiological explorations can be conducted at present [9]. Given mice's widespread

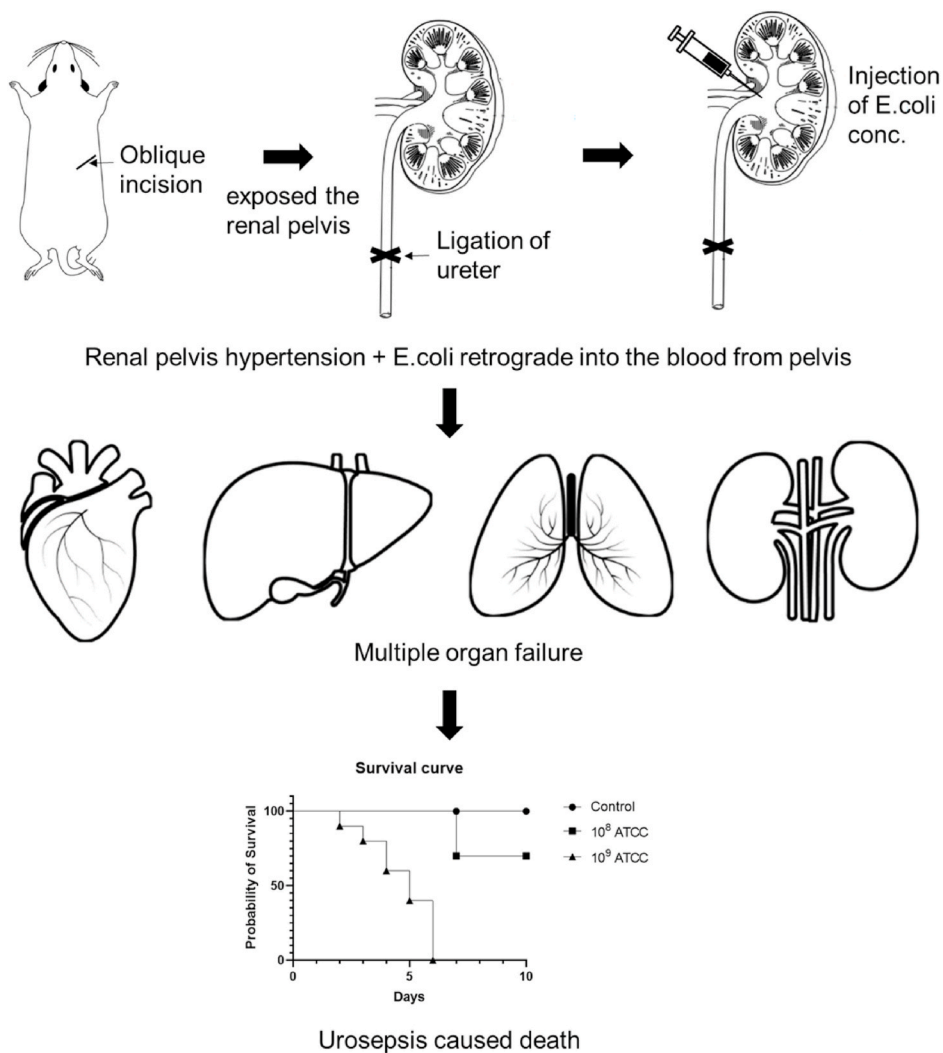


**Fig. 1.** Experimental procedure. Multiple organ failure was induced by ligation of ureter and injection of *Escherichia coli* into renal pelvis, and a stable urosepsis model was obtained.

use as model organisms in experimental research, a standardized mouse model of urosepsis would facilitate swift exploration of urosepsis' pathophysiological mechanisms.

Our study endeavored to create a consistent and replicable urogenic sepsis model in mice by ligating the ureter and administering *Escherichia coli* intrarenally in the renal pelvis. We gauged the soundness of the urosepsis model by monitoring survival rates, body temperature, symptomology scores, investigating changes in blood routine and inflammatory factors, and validating heart, lung, liver, and kidney's multi-organ impairment. This standardized mouse model of urosepsis has great potential in elucidating the underlying pathophysiological mechanisms of urosepsis, and provides valuable tools for identifying early diagnostic markers and treatment targets.

## 2. Materials and methods

### 2.1. Animal

We procured adult male C57BL/6J mice (weight: 25–30g, aged 9–10 weeks) from Beijing Spford Biotechnology Co. (Beijing, China) for our study. All experiments were conducted at the Animal Research Institute of Peking University Health Science Center after obtaining clearance from the Institutional Animal Care and Use Committee of Peking University Health Science Center (Animal Protocol: BCJC0117). The mice were acclimatized to the laboratory conditions for 7 days in an environment with regulated humidity (45–55 %), temperature (21–25 °C), and a 12-h light/dark cycle.

### 2.2. Experimental procedures

In our study, we randomly divided 84 male C57BL/6J mice into three groups based on the concentration of *Escherichia coli* solutions injected into their renal pelvis: Sham (injected with saline), Low-grade sepsis (injected with  $1.0 \times 10^8$  cfu/mL *E. coli*), and High-grade sepsis (injected with  $1.0 \times 10^9$  cfu/mL *E. coli*). Preceding the experiment, the mice underwent an overnight fasting period with unrestricted access to water. To begin the experiment, the mice were anesthetized by 1 % sodium pentobarbital (50 mg/kg, i.p.) [11,12].

After anesthesia, we sterilized the right abdominal skin of the mice with 75 % alcohol. We made a 0.5 cm oblique incision along the right costal margin 0.5 cm below, separated the epidermis and muscle layer to expose the kidney, without touching it. Then, the kidney

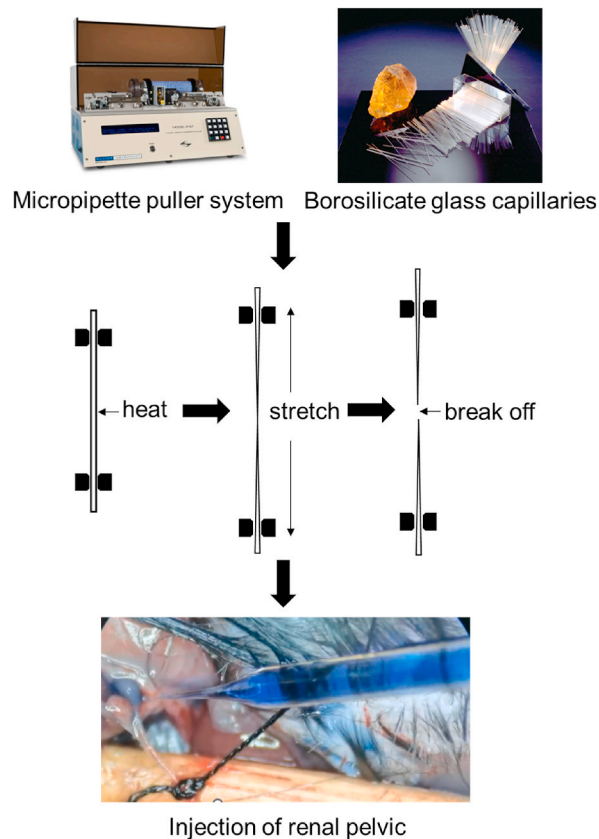


**Fig. 2.** The preparation process of glass needle. The preparation of glass needles can refer to the patch clamps preparation process. The glass needle prepared by this method can avoid bacterial outflow from the renal pelvis.

was gently extruded by applying steady, gentle pressure to the abdomen with the fingers [13]. Subsequently, we exposed the mouse ureter, ligated it with 4-0 silk 0.5 cm from the renal pelvis, exposed the renal pelvis, and injected a 100  $\mu$ L microsyringe (Gaoge Industry and Trade Co., Shanghai, China) combined with a glass needle (100  $\mu$ m in diameter) into the renal pelvis. The injection direction was horizontal towards the renal parenchyma. We injected Groups Low-grade sepsis and High-grade sepsis with 1 ml/kg of *E. coli* solution in the right renal pelvis at concentrations of  $1.0 \times 10^8$  and  $1.0 \times 10^9$  cfu/ml, respectively. We also injected 1 ml/kg of saline into the right renal pelvis of the control group. We ensured that all injection fluids were stained with trypan blue dye to confirm that there was no obvious leakage during the injection. After the injection, we sutured the mice and administered postoperative analgesic tramadol hydrochloride (10 mg/kg, s.c.) (Fig. 1).

In each group, 10 mice were selected for continuous monitoring of their activity scores postoperatively. Anal temperature measurements were taken at specific intervals (2h, 12h, 36h, and subsequently every 24h), and observations continued until euthanasia on the 10th day. Survival curves were then compiled based on the collected data.

Additionally, 18 mice were selected from each group for blood sampling at three postoperative time points (0h, 2h, 24h) via cardiac puncture. Some fresh blood samples were subjected to routine blood tests and blood cultures. The remaining blood samples were processed using a cryogenic centrifuge (CF1524R, SCILOGEX Co., USA) at 3000 rpm for 10 min, and the supernatant was stored at  $-80^\circ\text{C}$  for biochemical analysis. Simultaneously, after thorough perfusion with 0.01 mol/L PBS solution, tissues from the heart, liver, lungs, and kidneys were excised. The harvested tissues were fixed in 4 % paraformaldehyde and stored in a refrigerator at  $4^\circ\text{C}$ .

### 2.3. The preparation process of glass needle

The preparation of glass needles can refer to the patch clamps preparation process [14]: Firstly, insert a borosilicate glass capillary (Sutter instrument Co., USA) into the puller (P-97, Sutter instrument Co., USA) and heat it to a specific temperature. Then, use the puller to stretch the heated glass capillary, which will form a tapered tip at the middle of the capillary. Once the desired taper shape is achieved, stop pulling and let the glass cool down. Next, break off the glass capillary at the middle part to obtain a glass needle of the desired size (100  $\mu$ m diameter). Finally, clean the newly extracted glass needle with a mixture of nitric acid, hydrochloric acid, and ethanol to remove any impurities (Fig. 2).

### 2.4. Bacterial culture

*Escherichia coli*, abbreviated as *E. coli* (ATCC 25922) (Feimobio Co., Beijing, China) was cultivated on McConkey Agar (Sangon Biotech Co., Shanghai, China) for 24 h at a temperature of  $37^\circ\text{C}$  to allow for the formation of individual colonies. Subsequently, a solitary bacterium colony was selected and introduced into LB medium at  $37^\circ\text{C}$  with agitation at 200 revolutions per minute for a duration of 18–24 h. The bacterial medium underwent precipitation via centrifugation at 2000g for 10 min before being resuspended in saline to achieve a concentration of  $1.0 \times 10^8$ ,  $1.0 \times 10^9$  cfu/mL. In order to ensure accurate measurement of bacterial concentrations, bacterial suspensions underwent evaluation utilizing a bacterial turbidimeter (Thermo Fisher Scientific, USA).

Following the inoculation of *E. coli* for 24 h, blood samples were introduced onto MacConkey agar for 24 h at  $37^\circ\text{C}$ . The presence of pink colonies confirmed the existence of *E. coli* in the blood.

### 2.5. Physical observations

Following the intrapelvic injection of *Escherichia coli* into the renal pelvis, mice were subjected to a general response assessment at 2h, 12h, 36h, and subsequently every 24h. The assessment encompassed consciousness, activity, weakness, and mortality rates, concomitant with anal temperature measurements. Mice were euthanized once their behavior score reached 1, whereby 1 indicated a state of Moribund, in accordance with the methodology described by Yang et al. [15]. Euthanasia was executed via intraperitoneal injection of a 1 % dose of sodium pentobarbital at 250 mg/kg [16,17].

### 2.6. Blood routine and biochemical tests

The White Blood Cell (WBC) counts and Blood Platelet Counts (PLT) were analyzed using an automatic hematology analyzer (Thermo Fisher Scientific, USA). Meanwhile, heart function (measured via CK and LDH levels), liver function (measured via AST and ALT levels) and renal function (measured via BUN and CRE levels) were evaluated employing an automatic biochemical analyzer (Catalyst One, IDEXX Laboratories Co., Maine, USA).

### 2.7. Real-time PCR

As per the manufacturer's specifications, total RNA was extracted from various tissues (heart, liver, lung, and renal) utilizing the Tissue RNA Purification Kit Plus (ESscience Biotech, Shanghai, China). The quantification of RNA was performed at 260 nm/280 nm using the NanoDrop (Thermo NanoDrop 2000, Thermo Fisher Scientific Co., MA, USA). Following the package instructions, 2 mg of total RNA underwent reverse transcription to cDNA with the assistance of ABScript II RT Master Mix (ABclonal, Wuhan, China). Quantitative reverse transcription-polymerase chain reaction (qRT-PCR) was carried out on a Bio-Rad (Hercules, CA, USA) CFX96 system utilizing SYBR green to determine the mRNA expression level of the gene of interest. The primer sequence is outlined in Table S1. GAPDH was employed as an internal reference control for normalization, and the relative mRNA expression level for each

target gene was assessed using the  $2^{-\Delta\Delta CT}$  method.

## 2.8. Western blotting analysis

The tissues underwent complete lysis in RIPA buffer supplemented with 1 % protease inhibitor and 1 % PMSF, both sourced from Sigma-Aldrich (St. Louis, MO). A total of 200  $\mu\text{g}$  protein underwent separation through 10–12.5 % SDS-PAGE electrophoresis and was subsequently transferred onto a polyvinylidene fluoride membrane (Millipore, IPVH00010). Following a 1-h blocking step with 5 % skim milk at room temperature, the membrane was initially probed with the primary antibody overnight at 4 °C (Table S2). Subsequently, it was incubated with the secondary antibody (Table S3), at room temperature for an additional 1 h. Then, the bands on the membrane were visualized and detected using the iBright imaging system (FL1500, Thermo Fisher Scientific Co., MA, USA).

## 2.9. Hematoxylin and eosin (HE) staining

Heat the tissues that are embedded in paraffin on a hot plate at a high temperature of 60 °C for over 4 h to ensure proper adherence

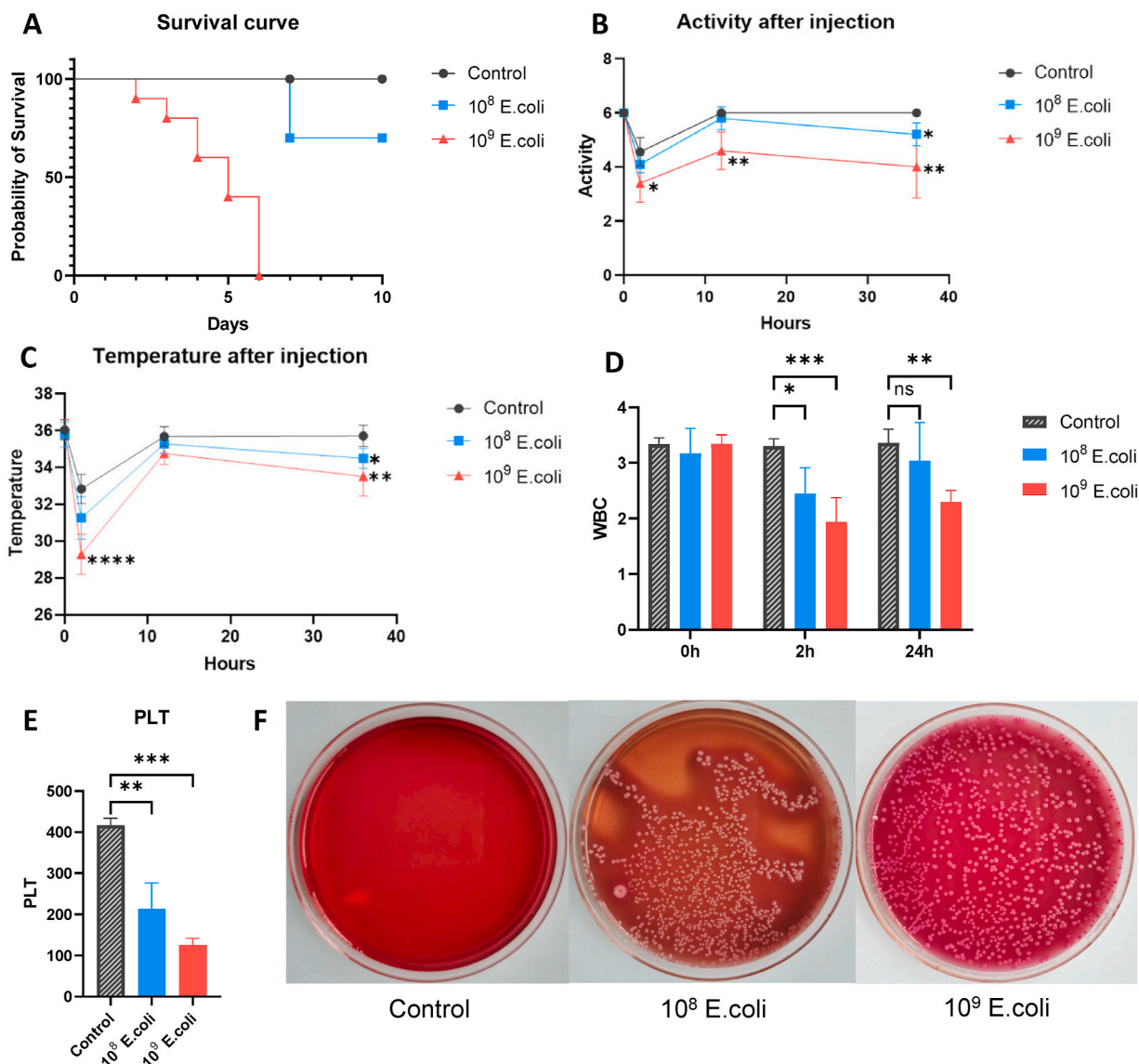


**Fig. 3.** Characterization of urosepsis in mice. (A) Survival analysis after ureter ligation and inoculation of *E. coli*. (B) Changes in activity score after modeling. (C) Changes in anal temperature after modeling. (D) Changes in WBC after modeling. (E) Changes in PLT after 24h of modeling. (F) Blood specimens were incubated on MacConkey agar at 37 °C after 24h inoculation with *E. coli*. Values were shown as mean  $\pm$  SD. \* $P < 0.05$ , \*\* $P < 0.01$ , \*\*\* $P < 0.001$ , and \*\*\*\* $P < 0.0001$  vs control group.

to the slides and facilitate enhanced deparaffination. Proceed to submerge the sample-laden slides in xylene twice, with each submergence lasting for approximately 30 min. Then, dip the slides consecutively in anhydrous ethanol, followed by 95 %, 85 %, and 75 % alcohol, concluding with deionized water for 5 min each. Submerge the tissues in a hematoxylin staining receptacle for approximately 10 min. Subsequently, delicately rinse them under flowing water for 5 min. Immerse the slides in an eosin staining receptacle for 10 s before subjecting the samples to dehydration in solutions of 75 %, 85 %, 95 %, and anhydrous ethanol, each time for 5 min. Render the tissue sections transparent by immersing them in xylene for 5 min. Finally, secure the section by applying around 60  $\mu$ L of neutral resin drops and carefully positioning the cover slide onto the section.

### 2.10. Immunohistochemical (IHC)

Tissue sections fixed with paraformaldehyde and embedded in paraffin were initially subjected to deparaffinization. Subsequently, endogenous peroxidase activity was suppressed using hydrogen peroxide. Antigen retrieval was accomplished through microwave irradiation. The specified primary antibody (Table S2) and secondary antibody (Table S3) were applied to the sections following the recommended protocols provided by the manufacturer. All slides were scrutinized under an inverted microscope at a magnification of 200  $\times$ .

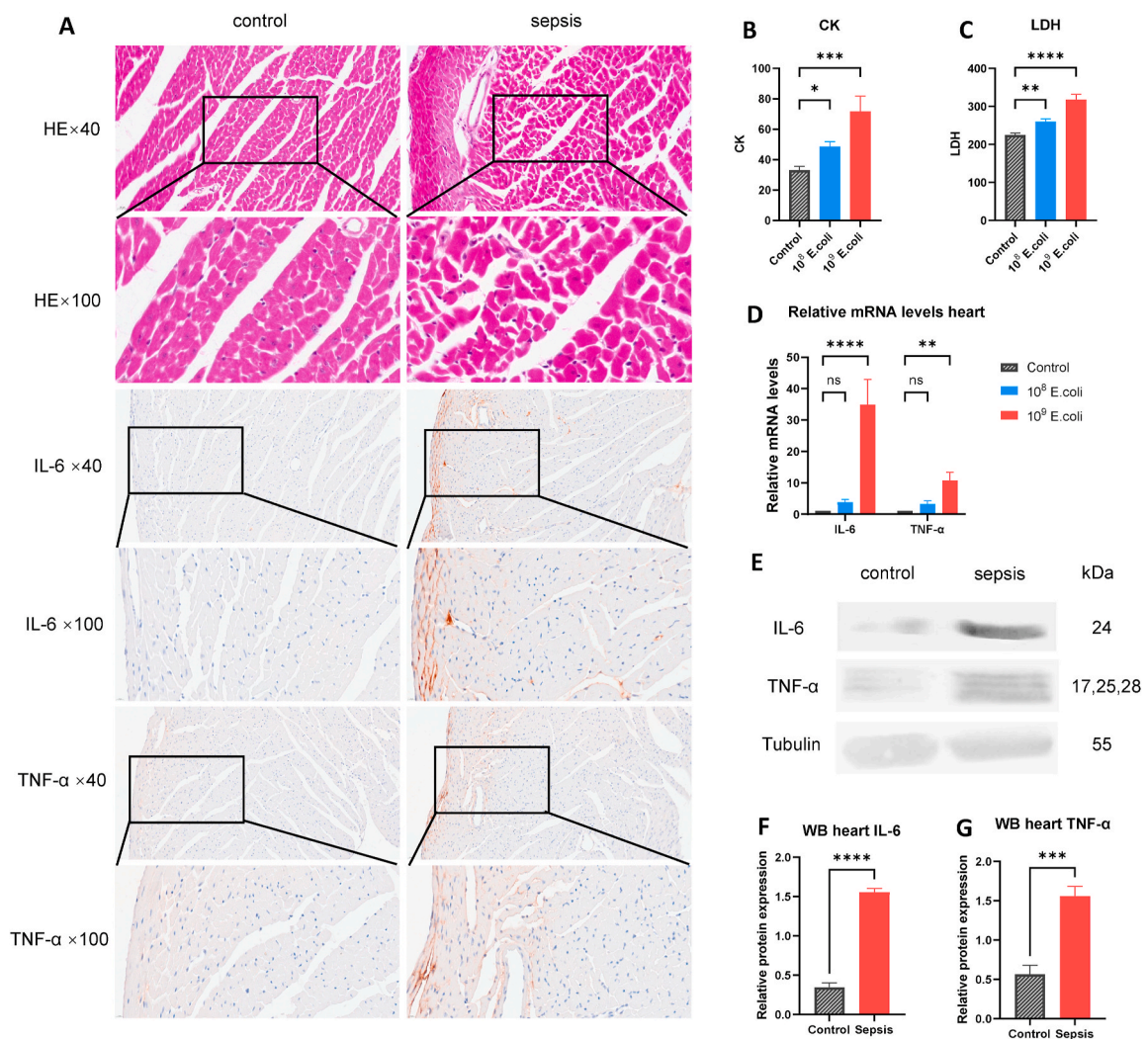


**Fig. 4.** Heart injury in the mouse model of urosepsis. (A) Representative images of hematoxylin and eosin (H&E) staining of heart tissue from the control and sepsis groups, immunohistochemical analysis of IL-6 and TNF- $\alpha$  in heart tissue. (B, C) Serum CK and LDH levels in mice 24 h after *E. coli* or saline inoculation of the renal pelvis. (D) The relative mRNA levels of IL-6 and TNF- $\alpha$  in the heart tissue. (E) Expressions of IL-6 and TNF- $\alpha$  in heart tissue were tested by Western blot, and b-tubulin was used as a loading control. (F, G) Quantitative data of the levels of IL-6 and TNF- $\alpha$ . Values were shown as mean  $\pm$  SD. \* $P < 0.05$ , \*\* $P < 0.01$ , \*\*\* $P < 0.001$ , and \*\*\*\* $P < 0.0001$  vs control group. "ns" means "not significant".

### 2.11. Statistical analysis

All experimental data were presented as means  $\pm$  standard error. Statistical analyses were conducted using Student t-tests or one-way ANOVA, with  $P < 0.05$  deemed to represent statistical significance.

## 3. Results

### 3.1. Surgical methods and critical points of the mouse urosepsis model

To investigate the mechanisms underlying urosepsis, we endeavored to establish a mouse urosepsis model (Fig. 1). Briefly, we performed right ureter ligation and subsequently delivered a limited volume of *E. coli* via renal pelvic injection using a fine glass needle (Fig. 2), in order to prevent bacterial outflow from the renal pelvis. Six mice were sacrificed at 0h, 2h, and 24 h after surgery to evaluate the model by collecting blood and organs, while the remaining 10 mice were monitored for survival. We encountered significant difficulty in establishing the urosepsis model due to the slender dimensions of the mouse renal pelvis and ureter, which had a width of approximately 1 mm. Standard 32G puncture needles have an external diameter of around 0.23 mm with beveled edges, necessitating that the bevel of the needle is entirely within the renal pelvis prior to injection. However, even slight instability during puncture could cause damage to and rupture of the renal pelvis, resulting in fluid leakage. During pre-experimental work, we discovered that using

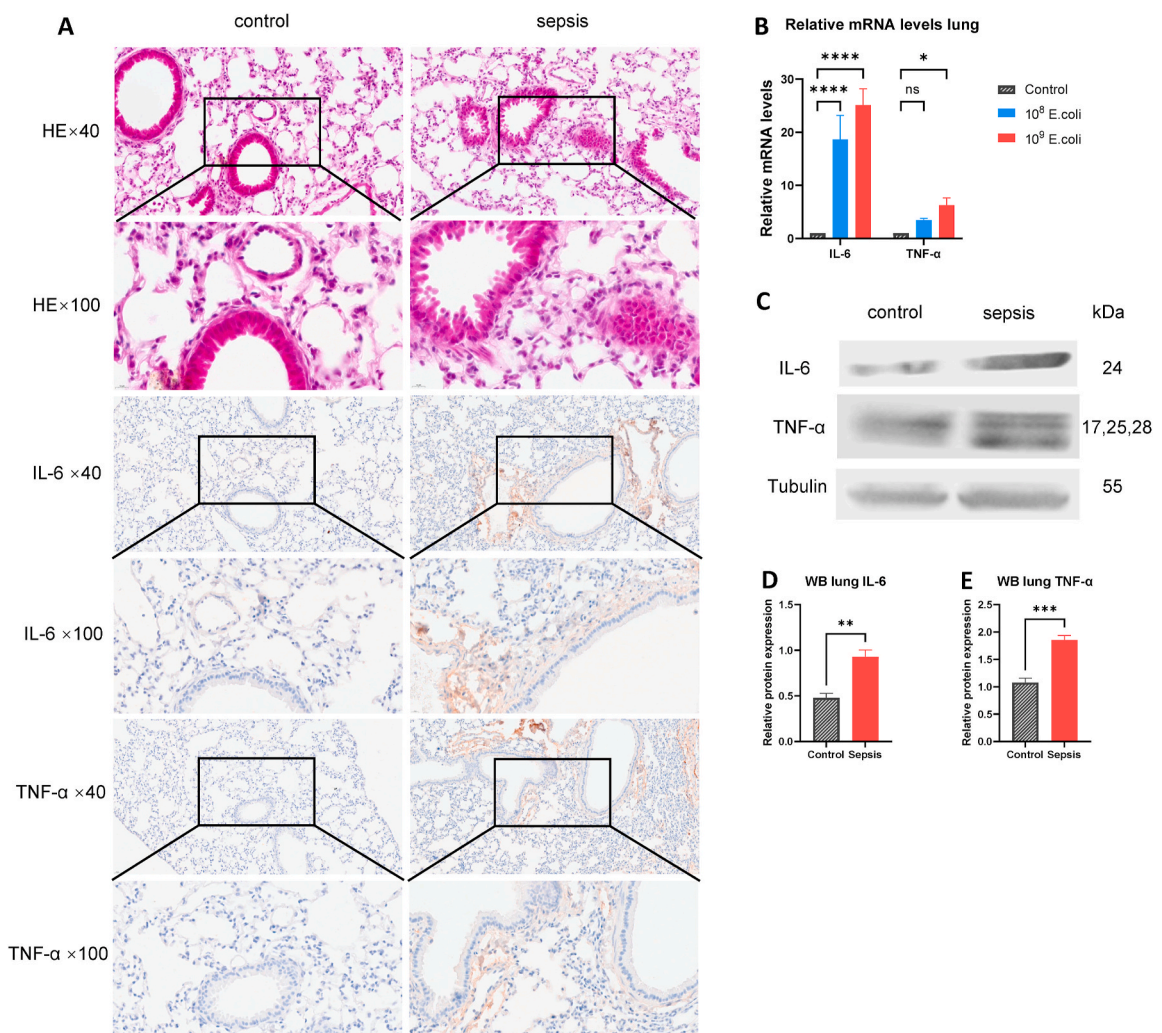


**Fig. 5.** Lung injury in the mouse model of urosepsis. (A) Representative images of hematoxylin and eosin (H&E) staining of lung tissue from the control and sepsis groups, immunohistochemical analysis of IL-6 and TNF- $\alpha$  in lung tissue. (B) The relative mRNA levels of IL-6 and TNF- $\alpha$  in the lung tissue. (C) Expressions of IL-6 and TNF- $\alpha$  in lung tissue were tested by Western blot, and b-tubulin was used as a loading control. (D, E) Quantitative data of the levels of IL-6 and TNF- $\alpha$ . Values were shown as mean  $\pm$  SD. \* $P < 0.05$ , \*\* $P < 0.01$ , \*\*\* $P < 0.001$ , and \*\*\*\* $P < 0.0001$  vs control group. "ns" means "not significant".

glass needles with a diameter of 100 μm proved effective in preventing leakage.

### 3.2. Characterization of urosepsis in mice

Our findings revealed that the renal pelvis injection of *E. coli* solution led to the demise of mice based on a 10-day survival analysis, and the fatality rate exhibited correlation with the concentration of the *E. coli*. Mortality stood at 30 % in the low-grade sepsis cohort and escalated to 100 % in the high-grade sepsis cohort (Fig. 3A). Concurrently, mice in the sepsis cohort displayed a reduction in activity scores and body temperature post-modeling, with notable distinctions manifesting within 36 h (Fig. 3B and C). Additionally, blood samples were procured at 0h, 2h, and 24h post-surgery, and the data demonstrated statistically significant alterations in WBC counts compared to preoperative values in all subjects, excluding the control group, following a 2-h renal pelvis injection of *E. coli* (Fig. 3D). The most pronounced changes were evident in the high-grade sepsis cohort, wherein the mean ± SD of the WBC count was  $1.94 \pm 0.44 \times 10^9/L$  (Fig. 3D). Similarly, the variation in PLT levels was most prominent in the high-grade sepsis, exhibiting a mean ± SD value of  $126.0 \pm 13.4 \times 10^9/L$  (Fig. 3E). Subsequent to a 24-h period post-*E. coli* or saline injection, blood cultures were conducted on all subjects, yielding positive results in the sepsis cohort and negative outcomes in the control group (Fig. 3F).

### 3.3. Heart injury in urosepsis mice

The High-grade sepsis group was compared to the control group, with tissue sections revealing obvious interstitial inflammatory

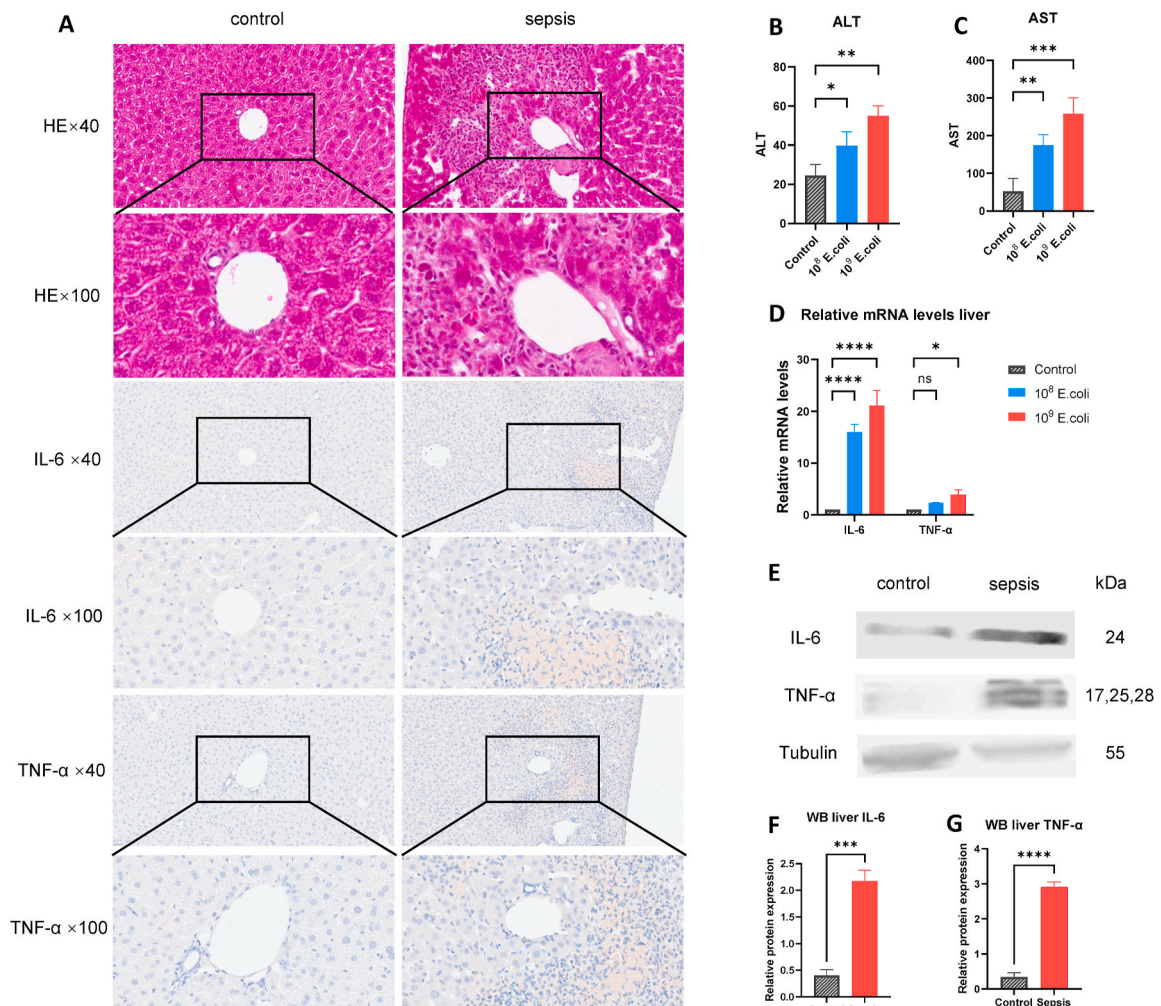


**Fig. 6.** Liver injury in the mouse model of urosepsis. (A) Representative images of hematoxylin and eosin (H&E) staining of liver tissue from the control and sepsis groups, immunohistochemical analysis of IL-6 and TNF-α in liver tissue. (B, C) Serum ALT and AST levels in mice 24 h after *E. coli* or saline inoculation of the renal pelvis. (D) The relative mRNA levels of IL-6 and TNF-α in the liver tissue. (E) Expressions of IL-6 and TNF-α in liver tissue were tested by Western blot, and b-tubulin was used as a loading control. (F, G) Quantitative data of the levels of IL-6 and TNF-α. Values were shown as mean ± SD. \*P < 0.05, \*\*P < 0.01, \*\*\*P < 0.001, and \*\*\*\*P < 0.0001 vs control group. "ns" means "not significant".

infiltration and edema in the myocardium of the sepsis group (Fig. 4A). IHC analysis conducted on paraffin-embedded heart tissues demonstrated significantly elevated levels of IL-6 and TNF- $\alpha$ , particularly in the epicardium of the sepsis group as opposed to the control group (Fig. 4A). Concurrently, commonly used indicators for assessing cardiac function, CK and LDH, showed substantial increases in the sepsis group (Fig. 4B and C). Furthermore, there were statistically significant variations in IL-6 and TNF- $\alpha$  mRNA levels in heart tissues between the sepsis and the control group ( $p < 0.05$ ) (Fig. 4D). The protein expression levels of IL-6 and TNF- $\alpha$  were also found to be elevated in the heart tissue of the high-grade sepsis group when compared to the control group (Fig. 4E-G, S1-S3).

### 3.4. Lung injury in urosepsis mice

The histological examination of lung tissues in the sepsis group and the control group revealed notable differences. In the sepsis group, obvious inflammatory cell infiltration and even abscess formation were observed in the alveolar wall and cavity, and cilia of bronchial epithelial cells showed obvious atrophy and destruction (Fig. 5A). IHC analysis conducted on paraffin-embedded lung tissues showed a significant increase in the levels of IL-6 and TNF- $\alpha$  in the sepsis group compared to the control group. This increase was particularly pronounced in the vascular endothelium and bronchial epithelium (Fig. 5A). Moreover, the expression levels of IL-6 and TNF- $\alpha$  mRNA in lung tissues of the sepsis mice were found to be significantly different from those in the control group ( $p < 0.05$ ) (Fig. 5B). The expression levels of IL-6 and TNF- $\alpha$  proteins in lung tissue of the sepsis group were higher than those in the control group

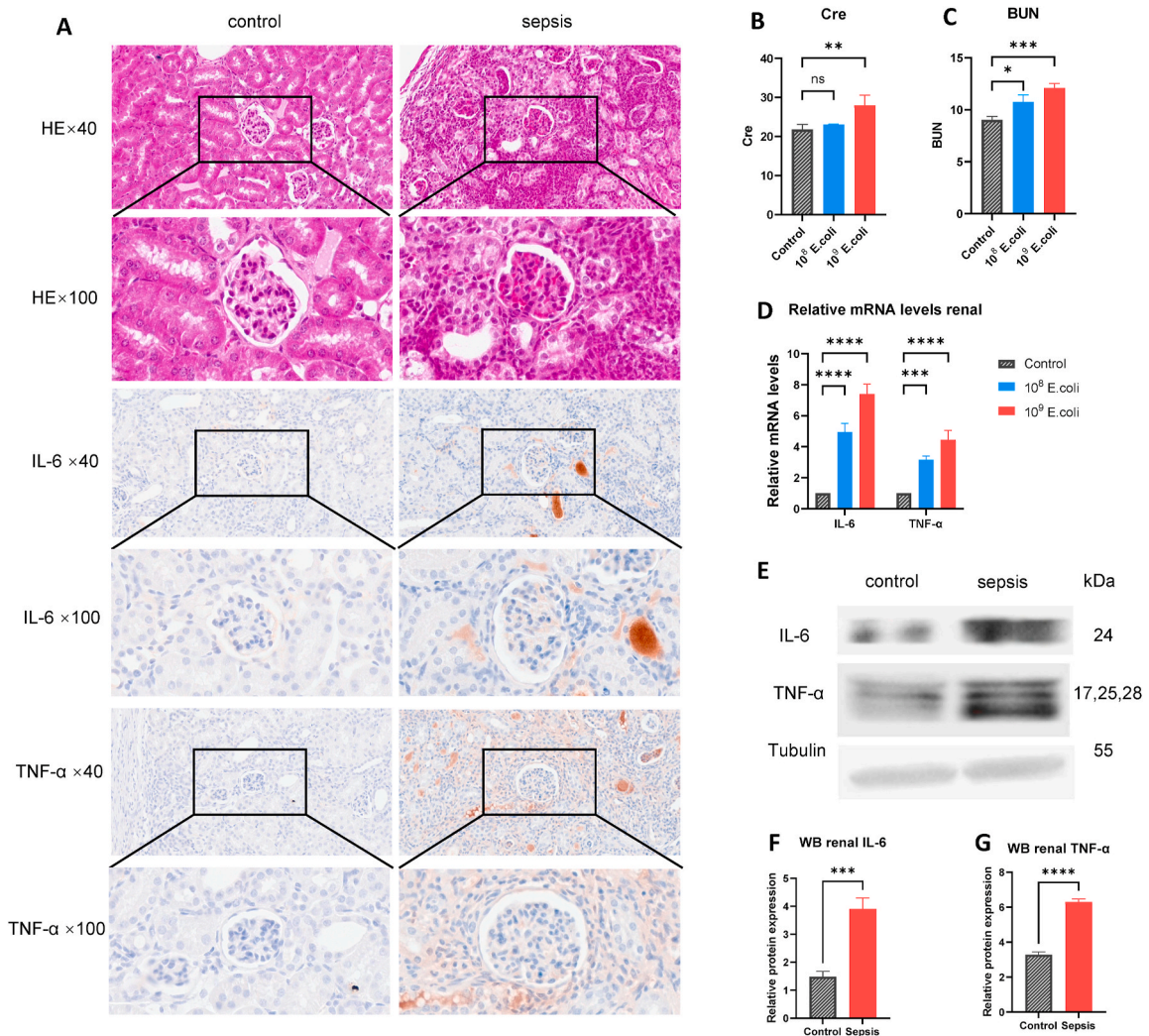


**Fig. 7.** Kidney injury in the mouse model of urosepsis. (A) Representative images of hematoxylin and eosin (H&E) staining of kidney tissue from the control and sepsis groups, immunohistochemical analysis of IL-6 and TNF- $\alpha$  in kidney tissue. (B, C) Serum Cre and BUN levels in mice 24 h after *E. coli* or saline inoculation of the renal pelvis. (D) The relative mRNA levels of IL-6 and TNF- $\alpha$  in the kidney tissue. (E) Expressions of IL-6 and TNF- $\alpha$  in kidney tissue were tested by Western blot, and b-tubulin was used as a loading control. (F, G) Quantitative data of the levels of IL-6 and TNF- $\alpha$ . Values were shown as mean  $\pm$  SD. \* $P < 0.05$ , \*\* $P < 0.01$ , \*\*\* $P < 0.001$ , and \*\*\*\* $P < 0.0001$  vs control group. "ns" means "not significant".

(Fig. 5C-E, S1-S3).

### 3.5. Liver injury in urosepsis mice

The histopathological examination of liver sections from septic mice provided insights into the liver injury associated with sepsis, including inflammatory infiltration, disordered cell arrangement, vacuolar necrosis, and duct hyperplasia (Fig. 6A). Multiple liver abscesses were also observed, and the expression of inflammatory factors at the abscess site was significantly increased (Fig. 6A). Furthermore, biochemical analysis indicated elevated serum levels of ALT and AST in the sepsis group, which suggested liver damage caused by sepsis (Fig. 6B and C). Besides, RT-PCR analysis of liver tissues showed a significant increase in the relative expressions of IL-6 and TNF- $\alpha$  mRNA in the sepsis group ( $p < 0.05$ ) (Fig. 6D). Western blot analysis also supported these findings (Fig. 6E-G, S1-S3).

### 3.6. Kidney injury in urosepsis mice

HE staining of right renal tissue in the sepsis mice revealed prominent characteristics of renal injury. Notable observations included vacuolar degeneration and necrosis of renal tubular epithelial cells, and extensive inflammatory cell infiltration (Fig. 7A). Additionally, the glomeruli exhibited significant erythrocyte blockage, while no erythrocyte or inflammatory cell infiltration was observed in the Bowman's capsule (Fig. 7A). IHC staining of kidney tissue further highlighted the extent of the inflammatory response, showing widespread overexpression of inflammatory factors (Fig. 7A). To assess kidney function, Cre and BUN levels were measured 24 h after injection. The results indicated elevated levels of both Cre and BUN in the sepsis group (Fig. 7B and C). Besides, RT-PCR analysis of mouse kidney showed that the relative mRNA levels of inflammatory cytokines were significantly higher than those of the control group (Fig. 7D). Finally, we found that the protein expression levels of IL-6 and TNF- $\alpha$  were significantly increased in the sepsis group compared with the control group by IHC and Western blot analysis of renal tissues (Fig. 7E-G, S1-S3).

## 4. Discussion

The study describes the establishment of a standardized mouse model of urosepsis through a specific procedure. The method involved ligating *E. coli* solution injected into the renal pelvis after unilateral ureter ligation. The experimental results indicate that we successfully achieved the objective of establishing a consistent urosepsis model in mice.

Over the past thirty years, the age-standardized incidence rate of sepsis has experienced a reduction of 37.0 %, and the mortality rate has decreased by 52.8 % globally [18]. Nonetheless, urosepsis constitutes 8.6 %–30.6 % of sepsis cases, with its incidence having significantly increased by 8.7 % annually, due to the widespread availability of upper urinary tract endoscopic surgeries [18–20]. In order to maintain a clear surgical field during the intracavity lithotripsy of the upper urinary tract, and to prevent thermal damage to the ureter caused by the crushing of stones, it is necessary to continuously infuse physiological saline into the ureter and renal pelvis. Bacteria present in the patient's urine and stones can rapidly enter the bloodstream due to high pressure in the renal pelvis during surgery, leading to some patients developing sepsis [3,21].

As a clinical syndrome with multiple organ failure as the main criterion, sepsis has complex and diverse etiologies, and the patient's disease progression can vary greatly, making it difficult to distinguish sepsis subgroups in clinical practice [22,23]. Nonetheless, urosepsis patients have characteristics such as a more concentrated pathogen type and a clear time of infection entry into the bloodstream (which is the time of renal pelvis perfusion during lithotripsy surgery for urosepsis patients) [21]. Therefore, there is great potential to discover corresponding early screening indicators and treatment targets. From this perspective, urosepsis is a worthy sepsis subclass to study. However, existing animal models cannot meet the current research status. The CLP mouse model, as the gold standard for sepsis animal models, has a modeling process that is closer to the perforation process of acute appendicitis in clinical practice, and does not reflect the pathological process of urosepsis very well [24]. In addition, although the urosepsis models based on rats and rabbits can reflect the bacterial entry into the bloodstream in urosepsis well, because rats and rabbits are not model organisms, there is a lack of corresponding transgenic animals and monoclonal antibodies in many key pathways studied, such as necrosis/apoptosis and HMGB1 [25], which are currently popular in sepsis research. Therefore, we believe that establishing a urosepsis mouse model is of great significance for studying the mechanism of post-lithotripsy urosepsis.

Presently, two aspects warrant consideration in understanding the mechanism of urosepsis following endoscopic lithotripsy. One aspect involves most patients with stones exhibiting bacterial infections in their urine, with *Escherichia coli* accounting for 43 % of such diagnoses [26]. On the other hand, continuous infusion of normal saline during the operation induces high pressure in the renal pelvis, leading to bacteria and endotoxin rapidly entering the bloodstream from the collecting system [27,28]. Wu et al. established a urosepsis model in New Zealand rabbits by injecting *E. coli* solutions into the ureter at a dose of 2 ml/kg to maintain intrapelvic hypertension [8]. Cao et al. demonstrated that a suitable sepsis model can be established by injecting a dosage of 3 ml/kg into the dilated ureter of Wistar rats, with the ureter ligated 24 h beforehand [10]. However, the ureter of mice is too thin, making it challenging to perform injections even after ligating the ureter beforehand. Therefore, we devised a mouse model of urosepsis referencing the operation of the mouse renal pelvis injection model. Preliminary experiments have shown that when using a regular insulin needle for intrapelvic injection, the relatively thick mouse ureter and the angled needle design can cause leakage by enlarging the puncture site, which cannot guarantee high pressure in the renal pelvis. Therefore, we refer to the patch clamp manufacturing method to produce glass needles with different diameters (50  $\mu\text{m}$ , 100  $\mu\text{m}$ , 150  $\mu\text{m}$ ) to connect to a microinjector [14]. Compared to regular insulin needles, these needles are thinner and less likely to damage the renal pelvis. Our pre-experiments have found that using a 100  $\mu\text{m}$  diameter needle for intrapelvic injection does not result in any noticeable Evans blue staining leakage, nor does it lengthen the

injection time due to a too-small needle diameter. After numerous attempts, we found that injecting 1 ml/kg of *E. coli* into the renal pelvis of mice can lead to rapid death. Autopsies on the dead mice showed enlarged right kidneys, thin renal parenchyma, intact renal cysts without rupture, confirming that the injection dosage meets the requirement of high pressure in the renal pelvis.

In our study, we observed a significant decrease in peripheral blood WBC count at 2 h after surgery in the High-grade sepsis group compared to the control group. This is consistent with previous studies that found a significant decrease in WBC counts 2 h after urogenic sepsis formation in rabbits and rats [8,10]. The main reason for the reduction in leukocyte level is likely due to the large amount of endotoxin that enters the bloodstream, causing leukocytes to adhere to the vascular wall and recruit to various organs and tissues [5,29]. At the same time, there was also a trend of decreased platelet levels, which reached a significant difference at 24 h. This may be related to the activation of the coagulation cascade caused by severe infection, leading to widespread platelet recruitment and the formation of disseminated thrombi, indicating the failure of coagulation function [30,31].

The host inflammatory response is a balancing act between proinflammatory and anti-inflammatory factors [6]. During the initial phases of sepsis, the activation of the host's innate immune system triggers the release of substantial quantities of pro-inflammatory mediators, encompassing IL-6 and TNF- $\alpha$ , along with diverse chemokines [32]. The expressions of IL-6 and TNF- $\alpha$  in various sepsis animal models exhibited a marked elevation compared to those in the normal group [33]. Our investigation discerned heightened expression levels of major inflammatory factors in multiple organs of urosepsis mice, culminating in pronounced dysfunction across various organs.

In 2016, the definition of sepsis was updated and this new definition places more emphasis on the severity of multiple organ damage, quantified by sequential organ failure assessment (SOFA) score [34]. The SOFA score includes six indicators, including oxygenation index, platelet count, bilirubin, mean arterial pressure, Glasgow coma scale and serum creatinine, to evaluate respiratory, coagulation, liver, cardiovascular, central nervous system and renal damage, respectively [35]. In our study, we found that septic mice had impaired coagulation function, mainly manifested as a decrease in platelet count. We also observed significantly higher levels of inflammatory factors in four different organs of the sepsis group compared to the control group, confirming damage to these organs in our mouse model of urosepsis.

Compared to existing animal models of urosepsis, such as New Zealand rabbits and Wistar rats, which lack effective research tools like antibodies against rabbits/rats and gene knockout animals, mice are the most widely used and do not require ligation of the ureter 24 h in advance for puncture. Skilled operators can establish the model for each mouse in just 20 min. Besides, good reproducibility of the model and lower feeding costs for mice are certainly advantageous factors for large-scale experiments. With further validation and optimization, this model can be widely used in the research and study of urosepsis (Table 1).

#### 4.1. Limitation of the study

However, the mouse model also has its limitations, notably the challenge of obtaining a limited volume of blood in a single extraction, making it difficult to consecutively draw blood at multiple time points without impacting mouse survival (Table 1). Despite mice being the most commonly utilized animal model, some studies suggest limitations in replicating genomic responses seen in human inflammatory diseases [36,37]. While many researchers unanimously regard animal studies as a fundamental component in improving patient outcomes, it's crucial to acknowledge the known limitations in translating findings from mice to humans clinically [38,39]. Any study involving mice merely represents the initial phase of an extensive process. Therefore, as we refine existing animal models based on these acknowledged limitations, subsequent validation steps need to be undertaken with caution.

## 5. Conclusion

Presently, extant animal models for urosepsis primarily rely on rabbits and rats, offering a representation of the pathogenesis inherent in human urosepsis. Nevertheless, the inherent constraints in effective research tools for rabbit/rat antibodies, gene knockout animals, and other indispensable investigative instruments impede the progression of mechanistic inquiries. In contrast, our investigation introduces an innovative mouse urosepsis model characterized by expedited modeling, enabling large-scale experiments, and authentically capturing the characteristics of the disease. This model affords researchers the opportunity to delve into diverse facets of urosepsis, encompassing the repercussions of inflammatory factors and organ impairment, thereby fostering the development of potential interventions for this menacing ailment.

**Table 1**  
Advantages and disadvantages of existing animal models of urosepsis.

Species	Advantages	Disadvantages	Range of application
Mouse	Short modeling time, Can be raised on a large scale, There are specific antibodies and gene knockout animals.	Low blood volume, Can not be sampled continuously.	Basic mechanism of urosepsis.
Rat	Can be sampled continuously.	Long modeling time (The ureter should be ligation 1 day in advance to ensure that the ureter is dilated).	Physiology of urosepsis.
New Zealand rabbit	Can be sampled continuously.	More expensive, Difficulty in large-scale feeding.	Physiology of urosepsis.

## Funding

The authors declare that no funds, grants, or other support were received during the preparation of this manuscript.

## Ethics approval

The studies involving laboratory animals were reviewed and approved by Institutional Animal Care and Use Committee (IACUC) of Peking University Health Science Center (Animal Protocol: BCJC0117).

## Data availability statement

Data associated with the study has not been deposited into a publicly available repository. Data will be made available on request.

## CRediT authorship contribution statement

**Haopu Hu:** Writing – original draft, Visualization, Validation, Methodology, Investigation, Formal analysis, Data curation. **Qiuxia Yan:** Writing – review & editing, Validation, Methodology, Investigation, Formal analysis, Data curation. **Xinwei Tang:** Resources, Project administration, Formal analysis. **Shicong Lai:** Supervision, Resources, Project administration. **Ziyu Qin:** Validation, Supervision, Software. **Tao Xu:** Supervision, Conceptualization. **Hong Zhang:** Writing – review & editing, Supervision, Methodology, Conceptualization. **Hao Hu:** Writing – review & editing, Supervision, Conceptualization.

## Declaration of competing interest

The authors declare that they have no known competing financial interests or personal relationships that could have appeared to influence the work reported in this paper.

## Appendix A. Supplementary data

Supplementary data to this article can be found online at <https://doi.org/10.1016/j.heliyon.2024.e25522>.

## References

- [1] L. Evans, et al., Surviving sepsis campaign: international guidelines for management of sepsis and septic shock 2021, *Intensive Care Med.* 47 (11) (2021) 1181–1247.
- [2] M.M. Levy, et al., Outcomes of the Surviving Sepsis Campaign in intensive care units in the USA and Europe: a prospective cohort study, *Lancet Infect. Dis.* 12 (12) (2012) 919–924.
- [3] F.M.E. Wagenlehner, et al., Diagnosis and management for urosepsis, *Int. J. Urol. : Official Journal of the Japanese Urological Association* 20 (10) (2013) 963–970.
- [4] M. Cecconi, et al., Sepsis and septic shock, *Lancet (London, England)* 392 (10141) (2018) 75–87.
- [5] Y.-Y. Zhang, B.-T. Ning, Signaling pathways and intervention therapies in sepsis, *Signal Transduct. Targeted Ther.* 6 (1) (2021) 407.
- [6] D. Liu, et al., Sepsis-induced immunosuppression: mechanisms, diagnosis and current treatment options, *Military Medical Research* 9 (1) (2022) 56.
- [7] D. Rittirsch, et al., Immunodesign of experimental sepsis by cecal ligation and puncture, *Nat. Protoc.* 4 (1) (2009) 31–36.
- [8] H. Wu, et al., Early drastic decrease in white blood count can predict uroseptic shock induced by upper urinary tract endoscopic lithotripsy: a translational study, *J. Urol.* 193 (6) (2015) 2116–2122.
- [9] G. Ge, et al., Proteomic signature of urosepsis: from discovery in a rabbit model to validation in humans, *J. Proteome Res.* 20 (8) (2021) 3889–3899.
- [10] Y. Cao, et al., A novel model of urosepsis in rats developed by injection of *Escherichia coli* into the renal pelvis, *Front. Immunol.* 13 (2022) 1074488.
- [11] A. Tsukamoto, et al., Vital signs monitoring during injectable and inhalant anesthesia in mice, *Exp. Anim.* 64 (1) (2015) 57–64.
- [12] L. Carbone, J. Austin, Pain and laboratory animals: publication practices for better data reproducibility and better animal welfare, *PLoS One* 11 (5) (2016) e0155001.
- [13] L.E. Woodard, et al., Hydrodynamic renal pelvis injection for non-viral expression of proteins in the kidney, *J. Vis. Exp.* (131) (2018).
- [14] C.L. Hill, G.J. Stephens, An introduction to patch clamp recording, *Methods Mol. Biol.* (2021) 2188. Clifton, N.J.
- [15] B. Yang, et al., Traumatic injury pattern is of equal relevance as injury severity for experimental (poly)trauma modeling, *Sci. Rep.* 9 (1) (2019) 5706.
- [16] J.W. Dutton, et al., Assessment of pain associated with the injection of sodium pentobarbital in laboratory mice (*Mus musculus*), *JAALAS : JAALAS* 58 (3) (2019) 373–379.
- [17] N.H. Shomer, et al., Review of rodent euthanasia methods, *JAALAS : JAALAS* 59 (3) (2020) 242–253.
- [18] K.E. Rudd, et al., Global, regional, and national sepsis incidence and mortality, 1990–2017: analysis for the Global Burden of Disease Study, *Lancet (London, England)* 395 (10219) (2020) 200–211.
- [19] G.S. Martin, et al., The epidemiology of sepsis in the United States from 1979 through 2000, *N. Engl. J. Med.* 348 (16) (2003) 1546–1554.
- [20] A.A. Grosso, et al., Intraoperative and postoperative surgical complications after ureteroscopy, retrograde intrarenal surgery, and percutaneous nephrolithotomy: a systematic review, *Minerva Urology and Nephrology* 73 (3) (2021) 309–332.
- [21] N.M. Dreger, et al., Urosepsis—Etiology, diagnosis, and treatment, *Deutsches Arzteblatt International* 112 (49) (2015).
- [22] E. Abraham, Moving forward with refinement of definitions for sepsis, *Crit. Care Med.* 49 (5) (2021) 861–863.
- [23] K.M. DeMerle, et al., Sepsis subclasses: a framework for development and interpretation, *Crit. Care Med.* 49 (5) (2021) 748–759.
- [24] L. Dejager, et al., Cecal ligation and puncture: the gold standard model for polymicrobial sepsis? *Trends Microbiol.* 19 (4) (2011) 198–208.
- [25] Y. Ren, et al., Discovery of a highly potent, selective, and metabolically stable inhibitor of receptor-interacting protein 1 (RIP1) for the treatment of systemic inflammatory response syndrome, *J. Med. Chem.* 60 (3) (2017) 972–986.
- [26] F.M.E. Wagenlehner, et al., Epidemiology, definition and treatment of complicated urinary tract infections, *Nat. Rev. Urol.* 17 (10) (2020) 586–600.

- [27] W. Zhong, et al., Does a smaller tract in percutaneous nephrolithotomy contribute to high renal pelvic pressure and postoperative fever? *J. Endourol.* 22 (9) (2008) 2147–2151.
- [28] G. Zeng, et al., International Alliance of Urolithiasis guideline on retrograde intrarenal surgery, *BJU Int.* 131 (2) (2023) 153–164.
- [29] T. Skirecki, J.-M. Cavaillon, Inner sensors of endotoxin - implications for sepsis research and therapy, *FEMS (Fed. Eur. Microbiol. Soc.) Microbiol. Rev.* 43 (3) (2019) 239–256.
- [30] S. Gando, et al., A multicenter, prospective validation study of the Japanese Association for Acute Medicine disseminated intravascular coagulation scoring system in patients with severe sepsis, *Crit. Care* 17 (3) (2013) R111.
- [31] R. Pawlinski, et al., Hematopoietic and nonhematopoietic cell tissue factor activates the coagulation cascade in endotoxemic mice, *Blood* 116 (5) (2010) 806–814.
- [32] S. Mera, et al., Multiplex cytokine profiling in patients with sepsis, *APMIS : Acta Pathologica, Microbiologica, Et Immunologica Scandinavica* 119 (2) (2011) 155–163.
- [33] J.-L. Li, et al., Assessment of clinical sepsis-associated biomarkers in a septic mouse model, *J. Int. Med. Res.* 46 (6) (2018) 2410–2422.
- [34] M. Singer, et al., The third international consensus definitions for sepsis and septic shock (Sepsis-3), *JAMA* 315 (8) (2016) 801–810.
- [35] S. Lambden, et al., The SOFA score-development, utility and challenges of accurate assessment in clinical trials, *Crit. Care* 23 (1) (2019) 374.
- [36] J. Seok, et al., Genomic responses in mouse models poorly mimic human inflammatory diseases, *Proc. Natl. Acad. Sci. U.S.A.* 110 (9) (2013) 3507–3512.
- [37] T. Shay, et al., Conservation and divergence in the transcriptional programs of the human and mouse immune systems, *Proc. Natl. Acad. Sci. U.S.A.* 110 (8) (2013) 2946–2951.
- [38] M.F. Osuchowski, et al., Abandon the mouse research ship? Not just yet!, *Shock* 41 (6) (2014) 463–475.
- [39] K. Takao, T. Miyakawa, Genomic responses in mouse models greatly mimic human inflammatory diseases, *Proc. Natl. Acad. Sci. U.S.A.* 112 (4) (2015) 1167–1172.